

Missing link between the 2D Quantum Hall problem and 1D quasicrystals

Anuradha Jagannathan

Laboratoire de Physique des Solides, Université Paris-Saclay, 91405 Orsay, France

(Dated: February 2023)

This paper discusses a connection between two important classes of materials, namely quasicrystals and topological insulators as exemplified by the Quantum Hall problem. It has been remarked that the quasicrystal “inherits” topological properties from the 2D Quantum Hall model. We show this explicitly by introducing the Fibonacci-Hall model as a link between a 1D quasicrystal and the magnetic problems. We show here how Chern numbers for bands in periodic approximants of quasicrystals can be computed, along with gap labels. The Chern numbers are thus seen as a consequence of a flux parameter ϕ^S induced by the geometry of winding in 2D space of the quasicrystal. We show the existence of lines of Lifshitz transitions in the phase space of the model. These are marked by change of Chern number and disappearance of edge states. The proposed extrapolation method can be generalized to higher dimensional 2D and 3D quasicrystals, where higher order Chern numbers could be computed, and related to experimentally measurable transport quantities.

I. INTRODUCTION

It is well-known that, while quasicrystals have no periodicity in real space, they can be obtained by projecting down from a higher dimensional periodic lattice. Topological band structures in quasicrystals have been a topic of active study in recent years. Most of these studies discuss topological properties which are extrinsic – for example, induced by magnetic field [1], or spin-orbit and other couplings [2–6]. In contrast, this paper considers the intrinsic topological properties of quasicrystals, arising solely due to their structure. A connection between the simplest quasicrystal, the Fibonacci chain and the 2D Quantum Hall (QH) problem embodied by the Harper [7] and Aubry-Andre models [8] has been pointed out [9] and generalized [10]. While such a relation exists formally, a correspondence between the 1D and 2D problems has not so far been made explicitly. In this paper, we introduce the Fibonacci-Hall model, as a candidate for the missing link between the two problems. It provides a new way to compute and to understand topological properties which govern physical properties of quasicrystals, such as transport, for example.

The class of quasiperiodic Hamiltonians covered in this paper are tight-binding single electron models with diagonal and off-diagonal terms of the form

$$H^{1D} = - \sum_{\langle i,j \rangle} t_i (c_i^\dagger c_{i+1} + h.c.) + \sum_i \epsilon_i c_i^\dagger c_i \quad (1)$$

where the parameters t_i and ϵ_i vary in space quasiperiodically. The spin indices have been suppressed as they do not play a significant role in our discussion. For almost periodic 1D systems, which include the above models, there is a “gap labeling theorem” due to Bellissard and coworkers [11] which states that all their spectral gaps can be indexed by integers – the gap labels. In the last decade or so of research on topological quasicrystals, the meaning of these gap labels has been clarified, and they have even been observed experimentally [12, 13]. In particular, the topological equivalence be-

tween the Fibonacci and the Aubry-André-Harper models was shown, and used in a topological pumping experiment [9]. We show by explicit construction of the Fibonacci-Hall Hamiltonian, that bands and gaps evolve continuously from the 2D QH band structure to those of the 1D quasicrystal. For finite periodic approximants, band Chern numbers are computed by a standard real space method due to Loring and Hastings [14]. We show that the gap labels deduced from the band Chern numbers are consistent with known values deduced using the gap labeling theorem. The phase space of the model has a Lifshitz type transition. In the open system, we show that edge states appear in the topological region of the phase diagram and that they disappear at the topological transition into the trivial state.

The connection between 1D and 2D is shown here for the case of the Fibonacci quasicrystal which based on the golden mean. It can be readily generalized to other 1D quasicrystals, notably those based on the so-called metallic means [15]. More interestingly the quasicrystal-Quantum Hall correspondence could in principle be extended to higher dimensional quasiperiodic tilings. It would be interesting to investigate their connection to a 4D Quantum Hall problem. The links between the two systems would allow for direct computations of higher order Chern numbers, with implications for non-linear transport coefficients that could be experimentally measured.

II. THE FIBONACCI, QUANTUM HALL AND FIBONACCI-HALL MODELS

In the cut-and-project method, the Fibonacci chain is obtained by projecting a set of points of the square lattice. These are points that lie within a strip S of slope of $1/\tau$, where $\tau = (\sqrt{5} + 1)/2$ is the golden mean, and perpendicular cross-section W , as shown in Fig.1a). The quasicrystal is had on projecting the selected points onto the x' axis (the direction of the strip). The slope may instead be a rational given by F_{k-2}/F_{k-1} , where F_k is

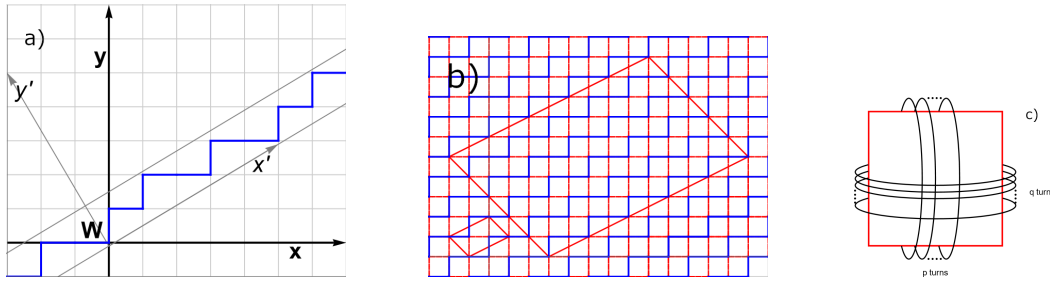


FIG. 1. a) Schema of the cut-and-project method. Selected points (joined by the zigzag blue line) lying in a strip \mathcal{S} of a 2D square lattice. These points are projected onto the x' axis to form the Fibonacci quasicrystal. The interval W represents the perpendicular cross-section of the strip corresponding to one unit square. b) The figure shows the parallel stacking of approximants in 2D for the approximant $N = 3$. A structural unit cell and the bigger magnetic unit cell are shown outlined in red. Intrachain bonds are colored blue, interchain bonds are colored red. c) Representation of an approximant chain, showing the wrapping of the rational cut around the unit torus, with winding numbers q and p along the x and the y directions respectively.

a Fibonacci number. This generates a periodic approximant having a unit cell of F_k sites, and the quasicrystal is obtained in the limit $k \rightarrow \infty$. The figure is drawn for a strip which passes infinitesimally below the origin O , but its position is arbitrary. If the strip is displaced parallel to itself, the zigzag blue line of selected points changes (“phason flips” occur). The origin of the unit cell is thereby changed, but the overall structure is not. Taking the vertical (resp. horizontal) hopping amplitudes to be t_b (resp. t_a) leads to a pure hopping model of the family H^{1D} , namely

$$H^F = - \sum_i t_i (c_i^\dagger c_{i+1} + h.c.) \quad (2)$$

where t_i is equal to t_a (t_b) for horizontal (vertical) bonds and the unit cell consists of F_k sites. In the following we will focus on this model, referred to as the “off-diagonal” Fibonacci model, although one notes that the approach could be modified to obtain other forms of H^{1D} . Many important results have been obtained for the Fibonacci models using their invariance under scale transformations combined with renormalization group (reviewed in [16]). The spectrum of the model Eq.2 has a distinctive hierarchical structure. The energy levels of the k th approximant have subgroups of levels, which in turn are composed of subgroups and so on. Spectra of larger approximants can be related to those of smaller approximants. The resulting gap structure is also hierarchical. The gap labeling theorem, as adapted for the k th periodic approximant [17]) states that the integrated density of states within the j th gap, $I_j^{(k)}$, can be written as

$$I_j^{(k)} = \left[g_j \frac{F_{k-1}}{F_k} \right], \quad (3)$$

where g_j is an integer ($|g_j| \leq F_k/2$) and where $[.]$ denotes the fractional part. Given any approximant all its gap labels can be readily computed using this formula.

Now, by extending the cut-and-project procedure to an infinite set of parallel strips, the entire 2D lattice can be regarded as an infinite set of parallel chains. Fig.1b) shows two unit cells of rhombic shape – the smaller rhombus is a structural unit cell for the $F_3 = 3$ approximant, while the larger rhombus is that of a magnetic cell as discussed below. Blue bonds connect sites along the *same* chain, and red bonds connect sites on neighboring chains. Fig.1c) is an equivalent compact representation of an periodic approximant corresponding to a slope p/q , showing the windings of the rational strip around the unit torus, q times and p along the x and the y directions respectively.

A 2D Quantum Hall Hamiltonian H^{2D} is now defined. To reproduce the Fibonacci winding property, a fictitious dimensionless flux $\phi^S = Ba^2/\phi_0$ is introduced, where B is a fictitious magnetic field perpendicular to the $x - y$ plane, a the side length and ϕ_0 the flux quantum. The superscript “S” indicates that this flux arises due to the winding property induced by the strip S . The flux ϕ_S has a different rational value for each approximant, as explained next. We first require that the total flux for the path shown in Fig.1c), namely, $(p + q)\phi^S$ be an integer. Thus, $\phi^S \propto (p + q)^{-1}$. The second requirement is to reproduce the hierarchical structure present in the spectra of Fibonacci chains, as seen by explicit computation in a perturbative limit [19–21]. For the Quantum Hall problem, there is an analogous result concerning sub-bands of the spectrum. A result obtained by Hofstadter [18] states that for a given rational flux f , the effective flux for sub bands is given by $[f^{-1}]$. If one sets $f = F_{k-1}/F_k$, then using the recursion relation for Fibonacci numbers, it is easy to see that

$$[f^{-1}] = \frac{F_{k-2}}{F_{k-1}} \quad (4)$$

in other words, the effective flux has a value associated with the next smallest approximant. This choice of flux maintains recursivity of the band structures as one goes from smaller to larger approximants. The flux is henceforth fixed to $\phi_k^S = F_{k-1}/F_k$ for the k th approximant.

In the quasiperiodic limit it converges to the (inverse) golden mean, τ^{-1} . Note that due to the symmetry of the problem under $\phi \rightarrow 1 - \phi$, an equivalent choice for the flux would be F_{k-2}/F_k .

Working in the Landau gauge with a vector potential $\vec{A} = (0, By, 0)$, the horizontal hopping terms are independent of the position. Vertical hopping amplitudes depend only on the x -coordinate of the bond. The resulting 2D Quantum Hall Hamiltonian can be expressed in the real space basis as

$$H^{2D} = \sum_{m,n} t_a c_{m+1,n}^\dagger c_{m,n} + h.c. + \sum_{m,n} t_b(m) c_{m,n+1}^\dagger c_{m,n} + h.c. \quad (5)$$

where c_{mn}^\dagger (c_{mn}) are the electron creation (destruction) operators on the lattice point $\vec{r}_{mn} = (m\vec{x} + n\vec{y})a$. The vertical hopping amplitudes are position dependent $t_b(m) = t_b e^{2i\pi m\phi^S}$ (dropping the subscript k in the flux for simplicity). Thanks to the chiral symmetry of the problem, one can consider t_a and t_b both to be positive, without loss of generality. To solve for the spectra, toroidal boundary conditions are imposed. The magnetic unit cell must be larger than the structural unit cell, to ensure the periodicity of hopping parameters from one cell to the next. This bigger cell is obtained by taking $N = F_k$ copies of the basic structural unit cell along each of the two directions defined by the basis vectors, as shown in Fig.1b). In this way one obtains the well-known QH energy spectrum consisting of N energy bands separated by $N - 1$ gaps (note that for even values of N two of the bands meet at $E = 0$).

In order to extrapolate from 2D to 1D limit, the inter-chain couplings between different chains are multiplied by a factor $0 \leq \epsilon \leq 1$. Fig.1b) shows the square lattice, with the intrachain bonds in blue, and inter-chain bonds in red. The resulting ϵ -dependent ‘‘Fibonacci-Hall’’ Hamiltonian is:

$$\begin{aligned} \langle i | H^{FH} | j \rangle &= \langle i | H^{2D} | j \rangle & i, j \in C \\ \langle k | H^{FH} | l \rangle &= \epsilon \langle k | H^{2D} | l \rangle & k \in C, l \in C' \neq C \end{aligned} \quad (6)$$

where the first relation holds for sites i and j that are located in the same chain (denoted by C), and the second line holds for sites located on two different chains.

To resume, H^{FH} depends on several parameters. The approximant size F_k , firstly, fixes the value of flux ϕ^S . The explicit parameters of the Hamiltonian are t_a , t_b and ϵ of which only two are independent, (we can set $t_a = 1$ without loss of generality). We will not discuss the extension of the model to include onsite potentials, but this could be done in an analogous way. There is an additional implicit parameter namely, the position of the selection strip. However this parameter has no incidence on the band structure when periodic boundary conditions

are applied. It does play a role in the energies of the edge states in an open system, discussed below.

A word about the H^{FH} model in the *absence* of ‘‘magnetic flux’’: it is topologically trivial but expected to have interesting electronic properties. It differs from the direct product of two identical Fibonacci chains (also called the square Fibonacci model) where the problem becomes separable along the two orthogonal directions [24, 25]. Using a well-known indexation [26] of sites using their so-called perpendicular coordinates, this 2D Hamiltonian has a rather simple Töplitz form (see S.I.).

III. PHASE DIAGRAM OF THE FIBONACCI-HALL MODEL

We are ready now to discuss the Fibonacci-Hall model in the $\epsilon - \delta$ parameter space, where $\delta = t_b - t_a$. The original 2D QH model is obtained for $\epsilon = 1$, while a set of identical decoupled Fibonacci Hamiltonians given by Eq.1 is obtained for $\epsilon = 0$. Both these limiting cases are well-understood. In all the following we will consider approximants, that is, periodic systems. The quasiperiodic limit $k \rightarrow \infty$ is understood for the limiting models. When $\epsilon = 0$, the 1D quasicrystalline model is critical for all $\delta \neq 0$, with multifractal spectrum and states (see the review in [16]). The 2D QH model is only critical for $\delta = 0$ [22], the isotropic case.

In the QH problem, a change occurs in the spectrum when one moves away from the isotropic limit $t_a = t_b$. This was shown by Zhang et al [23], by considering the semi-classical limit. For a range of energies, the Fermi surfaces open along one direction (giving rise to what they called ‘‘almost mobility edges’’ separating strongly localized from weakly localized states). In our present model, we have similar changes in the spectrum when ϵ is reduced for δ fixed. The first consequence of changing ϵ is a change of symmetry from square to rhombic (new tilted axes). Numerical results for the evolution of energy levels of H^{FH} for the $k = 4$ approximant are shown in Fig.2a). For clarity, we have shown the energy eigenvalues solved only at four special points $(0, 0)$, $(\pi, 0)$, $(0, \pi)$ and (π, π) in reciprocal space. These correspond to extremal states of the three bands, and are the energies for which band crossings occur as ϵ is varied. The figure shows level crossings as ϵ is decreased from 1.

As we will now explain, a level crossing can be interpreted as a variant of a Lifshitz transition. At this point, the zero flux constant energy surfaces near the crossing change in character from compact to extended – i.e. states evolve from being localized to extended along one direction. In our multigap system, states cross at different values of ϵ for each gap, with the main gap crossing occurring for the smallest value of ϵ . We now study the condition for the states to cross the main gap $g = \pm 1$, at $\epsilon = \epsilon_c$. The value of ϵ_c as a function of δ can be approximately computed as follows using a 3-band model and following the analyses in [23]. Indeed, the recursive

band structure of the Fibonacci system implies that the parent chain for the two main gaps is the 3-site approximant chain $t_a - t_a - t_b$. For zero flux, the Hamiltonian in the reciprocal space basis of this tilted system is given by a 3×3 matrix ,

$$\begin{pmatrix} 0 & 1 + \epsilon \rho e^{iK'} & e^{-iK} + \epsilon \rho e^{i(-K+K')} \\ 1 + \epsilon \rho e^{-iK'} & 0 & \rho + \epsilon e^{-iK'} \\ e^{iK} + \epsilon \rho e^{i(K-K')} & \rho + \epsilon e^{iK'} & 0 \end{pmatrix}$$

where $\rho = t_b/t_a = 1 + \delta$ and the reduced momentum components K and K' vary within $[0, \pi]$. Diagonalizing, one can get the three energy bands in momentum space, $E_j(K, K')$ ($j = 1, 2, 3$). Following these energies as a function of ϵ , one observes that there are band crossings. For example the lower band gap is traversed by two branches, $E_2(0, \pi)$ and $E_1(0, 0)$, that intersect for a certain value ϵ_c . The energy surfaces also show a change of form at this point, going from compact to extended surfaces in a form of Lifshitz transition. Series expansion for small ϵ and δ gives the solution $\epsilon_c \approx 2\delta/(3 + 2\delta)$. For larger δ one can solve for ϵ_c numerically. A study of the $k = 3$ and also bigger approximants shows similar behavior. For any system size, the following conjecture

$$\epsilon_c = \frac{\delta}{(\phi^S)^{-1} + \delta} \quad (8)$$

is well obeyed by the data (see S.I.). This novel form of Lifshitz transition has not been reported before to our knowledge. It is indicated in Fig.2b) by the dashed blue lines demarcating the topological and trivial regions.

Level crossings in the other gaps could, in principle, be similarly described via a theory utilizing suitably renormalized hopping parameters (discussed in the strong modulation limit in [19–21]). A complete study of all these transitions is outside the scope of this paper but we find that, just as for the main gap, no level crossings occur when $\delta = 0$. In this limit, it is possible to move adiabatically in the parameter space, as shown in the next section.

One can reach the off-diagonal Fibonacci chain model starting from the QH problem without any band crossings, for a finite system. Fig.2b) illustrates the corresponding path in the $\epsilon - \delta$ plane.

- With $\delta = 0$ fixed, ϵ is reduced from 1. There are no crossings except at $\epsilon = 0$. In finite systems ϵ is decreased to a small value $\epsilon_{min} \neq 0$ of the order of the typical energy level spacing. ϵ_{min} is small and decreases with system size.
- When the point A at $(\epsilon_{min}, 0)$ is reached, one goes from A to B at $(0, \delta_{min})$ (with $\delta_{min} \sim \epsilon_{min}$), thus avoiding the origin.
- From B, one goes along the vertical axis to the desired final value of δ .

Fig.2b) shows the path in parameter space and the evolution of bands along the path is shown in Fig.2c) for the

n	1	2	3	4	5	6	7	8	9	10	11	12	13
C_n	5	-8	5	-8	5	5	-8	5	5	-8	5	-8	5
g_n	5	-3	2	-6	-1	4	-4	1	6	-2	3	-5	

TABLE I. Upper row: the Chern numbers C_n of all the bands of H^{FH} (Eq.6) for system size $N = 13$. Lower row : the gap labels for each of the 12 gaps as deduced from the upper row. In the limit of an infinite system these values are independent of δ and ϵ for $0 \leq \epsilon \leq 1$.

$k = 4$ approximant. It can be seen that the gaps remain open all through. For purposes of clarity, in order to see gaps clearly, we have chosen a large value of $\epsilon_{min} = 0.2$.

The Chern numbers for each of the bands can be computed using the real space method due to Loring and Hastings [14]. Site positions \vec{r}_i are re-expressed as a pair of variables (θ_i, φ_i) in the range $[0, 2\pi)$. One defines the two diagonal Hermitian matrices $\Theta = \exp(i\theta)$ and $\Phi = \exp(i\varphi)$. Using the projection operators P_n , which project onto the n th band, one computes the matrices $U = P_n \Theta P_n$ and $V = P_n \Phi P_n$. For a large enough system size these are almost unitary because of the short range nature of the Hamiltonian [14]. The Chern number of the band is then given by

$$C_n = \frac{1}{2\pi} \text{Im}[\text{Tr} \text{Log}(VUV^\dagger U^\dagger)] \quad (9)$$

The gap labels are given by

$$g_n = \sum_{m=1}^n C_m \quad (10)$$

for $n = 1, \dots, n-1$. Table 1 lists the Chern numbers of the bands, and the gap labels which have been deduced from the Chern numbers for the $F_n = 13$ approximant. The gap labels we obtain in this way agree with the values determined using the gap labeling theorem Eq.3. To conclude, the Chern numbers arising due to the fictitious magnetic flux in two dimensions are seen to be related to the topological invariants of the 1D quasicrystal by adiabatic continuity.

IV. EDGE STATES. LIFSHITZ TRANSITION TO TRIVIAL STATE

In open systems the bulk-edge correspondence leads to edge modes. One can use the edge modes as markers for the various topological transitions in the $\epsilon - \delta$ plane. For these edge mode studies, we considered square unit cells

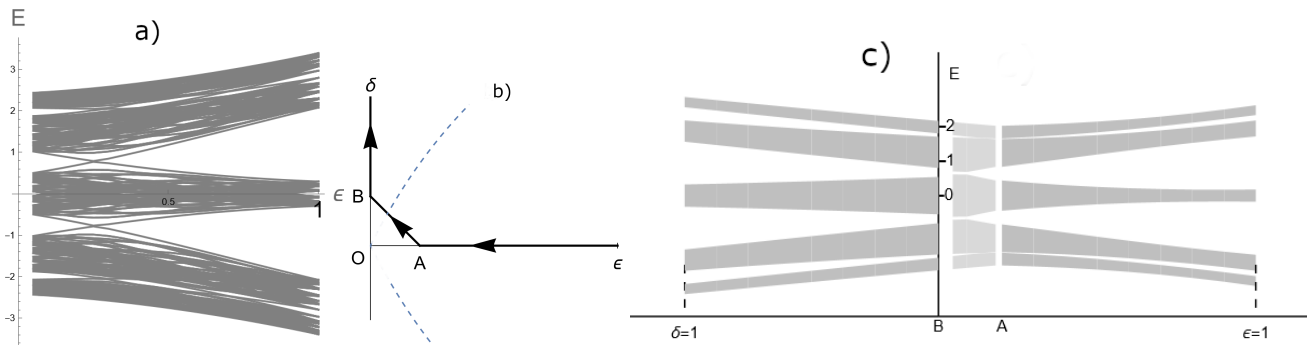


FIG. 2. a) The evolution of energy levels of H^{FH} as a function of ϵ , showing crossings for fixed $\delta = 0.5$. Data was obtained for $k = 4$ approximant (125 site magnetic unit cell) for four special points in reciprocal space $(0, 0)$, $(\pi, 0)$, $(0, \pi)$ and (π, π) . b) Schema of the path in δ - ϵ parameter space used for the plot in figure c). The point A corresponds to a relatively large value of $\epsilon_{min} = 0.2$ so that the gaps can be seen more clearly. The dashed blue lines indicate the Lifshitz transition for the main gap Eq.8. c) Evolution of bands and gaps of the Hamiltonian Eq.6 for a $N = 5$ approximant when going adiabatically from the isotropic QH model ($t_b = \epsilon = 1$) to the off-diagonal Fibonacci model with $\epsilon = 0$, $t_b = 2$.

(its characteristics are discussed in the S.I.) and solve for the eigenstates of Eq.6 when the long edges are left open, and periodic boundary conditions are applied along the y' direction. Here we will study edge states in the main gap. Let us start with $\epsilon = 1$, when one is in the topological sector, with an edge state in the gap. As ϵ is reduced, the edge state starts to extend further into the bulk. At some point a topological transition occurs with a corresponding change of the edge state. There is simultaneously a change of the Chern number, which drops to zero.

This evolution of edge states is shown in Fig.3(top). The computations are done for $\delta = 0.4$ and for a fixed band filling. The spatial profile of a state lying in the one of the big gaps (label $g = -1$) is shown using circles of size proportional to the onsite wavefunction amplitude. The state is shown for four different values of ϵ above and below the topological transition. The total Chern number of the first two bands for the case $\delta = 0.4$ is plotted in order to determine the point at which the transition occurs. This number, \mathcal{C} , plotted as a function of ϵ in Fig.3(bottom) shows that the transition occurs around $\epsilon = 0.2$, in agreement with the formula of Eq.8. Below this value, the edge state is no longer localized on the edge but instead is localized around a single chain. It now corresponds to a bulk 1D state.

The behavior of edge states thus follows what is expected by the principle of bulk-edge correspondence. They exist in the topological sector which is present for all values of δ , and $\epsilon > \epsilon_c$. They disappear in the trivial sector ($\epsilon < \epsilon_c$), states becoming localized on the chains instead. Finally, for $\epsilon = 0$, a variety of 1D edge states are seen in the decoupled chains as confirmed by experiments [12].

V. CONCLUSIONS

This paper considers the relation between the 2D Quantum Hall problem and 1D Fibonacci quasicrystals that has been pointed out in a number of pioneering studies [9], and proposes a “missing link” between them, the Fibonacci-Hall model. The Chern numbers are thus seen as a consequence of a flux parameter ϕ^S induced by the winding in 2D space of the quasiperiodic chain. This connection allows to clarify how the 1D quasicrystal can “inherit” topological properties from the 2D system. After describing its construction, and outlining its phase diagram, we compute its Chern numbers and from them deduce gap labels for the Fibonacci chain. The gap labels are in accord with those determined by the gap labeling theorem, and as verified by experimental investigations [12]. The topological invariants are robust with respect to perturbations providing that gaps do not close. For the finite Fibonacci chains, it is known that disorder conserves the gaps structure [33] – and therefore the gap labels – for sufficiently weak disorder. We also propose an exact relation for a Lifshitz transition which has not to our knowledge been studied before.

Similar extension to 2D can be readily carried out for other 1D quasicrystals, for example the silver mean and higher metallic mean chains. In future work, generalizing the present approach, it will be interesting to consider 2D quasicrystals, and their connection to a 4D Quantum Hall problem. One often-studied 2D example is the Ammann-Beenker tiling based on the silver mean [29, 30]. The spectral gaps for this tiling have been discussed in [31], along with a labeling scheme. In addition to the theoretical aspect, there are a number of additional physical properties that can be studied for higher dimensional topological systems. In particular, non-linear responses involving first and second Chern numbers could be computed explicitly for this case. It would be an extension to a real 2D case of the pioneering work of Lohse et al

[32] on quantized nonlinear transport in a synthetic 2D quasicrystal obtained by multiplying two Aubry-André chains. The quantized nonlinear conductances could be experimentally measured for real quasiperiodic systems.

VI. ACKNOWLEDGMENTS

I gratefully acknowledge many useful discussions with Pavel Kalugin, Frédéric Piéchon, Gilles Montambaux and Mark Goerbig.

-
- [1] J.N. Fuchs and Vidal, Phys. Rev. B **94**, 205437 (2016)
 - [2] H. Huang and F. Liu, Phys. Rev. Lett. **121**, 126401 (2018); Phys. Rev. B **98**, 125130 (2018)
 - [3] R. Chen et al, Phys. Rev. Lett. **124**, 036803 (2020)
 - [4] Cao et al, Phys. Rev. Lett. **125**, 017002 (2020)
 - [5] R. Ghadimi et al, Phys. Rev. B **104**, 144511 (2021)
 - [6] A. Kobialka, Phys. Rev. B **110**, 134508
 - [7] P. G. Harper, Proc. Phys. Soc., London, Sect. A **68**, 874 (1955)
 - [8] S. Aubry and G. Andre, Ann. Isr. Phys. Soc. **3**, 133 (1980)
 - [9] Y.E. Kraus et al, Phys. Rev. Lett. **109** (2012) 106402; M. Verbin et al, Phys. Rev. Lett. **110** (2013) 076403
 - [10] S. Ganeshan, K. Sun and S. das Sarma, PRL **110**, 180403 (2013)
 - [11] J. Bellissard, A. Bovier and J. M. Ghez, Rev. Math. Phys. **4** 1 (1992)
 - [12] D. Tanese et al, Phys. Rev. Lett. **112** 146404 (2014) ; F. Baboux et al, Phys. Rev. B **95**, 161114(R) (2017)
 - [13] A. Dareau et al, Phys. Rev. Lett. **119**, 215304 (2017)
 - [14] T. A. Loring and M. B. Hastings, Europhysics Letters **92**, 67004 (2010); T.A. Loring, Ann. Phys. (Amsterdam) **356**, 383 (2015)
 - [15] The golden, silver and other metallic means are irrational numbers that are solutions of the quadratic equation $x^2 - nx - 1 = 0$, for $n = 1, 2, \dots$
 - [16] A. Jagannathan, Rev. Mod. Phys. **93**, 045001 (2021)
 - [17] N. Mace et al, Journal of Physics: Conf. Series **809** 012023 (2017)
 - [18] D. R. Hofstadter, Phys. Rev. B **14**, 2239 (1976)
 - [19] Kalugin, Pavel A., Kitaev A. Yu. and Levitov, L. S., JETP vol.64, 410 (1986)
 - [20] Q. Niu and F. Nori, Phys. Rev. Lett. **57** 2057 (1986); Phys. Rev. B **42** 10329 (1990)
 - [21] F. Piechon et al, Phys. Rev. Lett. **74**, 5248 (1995)
 - [22] Artur Avila, Svetlana Jitomirskaya, Annals of Mathematics, Vol.170, Issue 1, Page 303 (2009).
 - [23] Y. Zhang et al, arXiv condmat 1504.05205 (2015)
 - [24] S. Even-Dar Mandel and R. Lifshitz, Phil. Mag. **88** 2261 (2008)
 - [25] S. Thiem and M. Schreiber, Eur. Phys. J. B **83**, 415 (2011)
 - [26] C. Sire and R. Mosseri, J. de Physique, **51** 1569 (1990)
 - [27] N. Macé, Anuradha Jagannathan, Pavel Kalugin, Rémy Mosseri, and Frédéric Piéchon, Phys. Rev. B, **96**, 045138 (2017).
 - [28] Baake, Michael and Grimm, Uwe, Aperiodic Order, Encyclopedia of Mathematics and its Applications, Cambridge University Press, 2013
 - [29] B. Grünbaum, G.C. Shepherd, Tilings and Patterns, W.H. Freeman, New York, 1987, p. 556.
 - [30] A. Jagannathan and M. Duneau, Isr. J. Chem. **64** e202300119 (2024)
 - [31] A. Jagannathan, Phys. Rev. B **108**, 115109 (2023)
 - [32] M. Lohse et al, Nature **553**, 55 (2018)
 - [33] A. Jagannathan, P. Jeena and M. Tarzia, Phys. Rev. B **99** 054203 (2019)

Supplementary Information

I. FIBONACCI-HARPER MODEL FOR ZERO FLUX

This section describes the Fibonacci-Harper model in zero magnetic field, $H_{\phi^S=0}^{FH}$. The Hamiltonian of Eqs. 5,6 and 7 of the main text can be written as the sum of two nearest neighbor Hamiltonians, $H_{\phi^S=0}^{FH} = H_{\parallel} + \epsilon H_{\perp}$. Here H_{\parallel} groups together the hopping terms along a given chain, and H_{\perp} the hopping terms between chains. A notable feature of this model is, that the roles of t_a and t_b are interchanged when going from the parallel to the perpendicular direction. A convenient basis to represent the Hamiltonian consists of using the so-called conumber basis, which numbers the sites according to increasing y' coordinates. One can write $H_{\phi=0}^{FH} = H_{\parallel} + \epsilon H_{\perp}$ as already described in the main text. H_{\parallel} is nothing but the Hamiltonian of a periodic approximant, which is known to have a Töplitz form [26]. With periodic boundary conditions along the chain, it is the $F_k \times F_k$ matrix

$$H_{\parallel} = \begin{pmatrix} 0 & t_a e^{iK} & \dots & t_b & \dots & & \\ & 0 & & t_a & \dots & t_b & \dots \\ & & 0 & & t_a & \dots & t_b & \dots \\ & & & & & \ddots & & \ddots \\ & & & & & & \ddots & \\ t_a e^{-iK} & & & & & & & \\ & t_a & & & & & & \\ & & t_a & & & & & \\ & & & t_b & & & & \\ & & & & t_b & & & \\ & & & & & \ddots & & \\ & & & & & & \ddots & \end{pmatrix} \quad (11)$$

where the only non-zero matrix elements, t_a and t_b , lie on diagonals located at distances F_{k-2} and F_{k-1} from the main diagonal. The reduced momentum variable K lies in the interval $[0, \pi]$. Similarly, H_{\perp} can be written as

$$H_{\perp} = \begin{pmatrix} 0 & \tilde{t}_b e^{iK} & \dots & \tilde{t}_a & \dots & & \\ & 0 & & \tilde{t}_b & \dots & \tilde{t}_a & \dots \\ & & 0 & & \tilde{t}_b & \dots & \tilde{t}_a & \dots \\ & & & & & \ddots & & \ddots \\ & & & & & & \ddots & \\ \tilde{t}_b e^{-iK} & & & & & & & \\ & \tilde{t}_b & & & & & & \\ & & \tilde{t}_b & & & & & \\ & \tilde{t}_a^* & & & & & & \\ & & \tilde{t}_a^* & & & & & \\ & & & & \ddots & & & \\ & & & & & \ddots & & \end{pmatrix} \quad (12)$$

with $\tilde{t}_a = t_a e^{iK'}$ where the momentum variable K' lies in the interval $[0, \pi]$.

As a result, the total Hamiltonian also has a rather simple Töplitz form. In particular, for $K = K' = 0$ one has

$$\begin{pmatrix} 0 & t_1 & \dots & t_2 & \dots & & \\ & 0 & & t_1 & \dots & t_2 & \dots \\ & & 0 & & t_1 & \dots & t_2 & \dots \\ & & & & & \ddots & & \ddots \\ & & & & & & \ddots & \\ t_1 & & & & & & & \\ \cdot & t_1 & & & & & & \\ \cdot & \cdot & t_1 & & & & & \\ t_2 & & & & & & & \\ & t_2 & & & & & & \\ & & \ddots & & & & & \\ & & & \ddots & & & & \end{pmatrix} \quad (13)$$

where $t_1 = t_a + \epsilon t_b$ and $t_2 = t_b + \epsilon t_a$.

The eigenvalues for this matrix are those of a 1D approximant chain with hopping parameters t_1 and t_2 . This leads to the conclusion that, at the origin $(K, K') = (0, 0)$, this spectrum will be multifractal for $t_1 \neq t_2$ in the $k \rightarrow \infty$ limit. The study of the full spectrum is left for future work.

Finally, note that for $\epsilon = 1$, this problem becomes translationally invariant and one has the standard dispersion relation $E(k_x, k_y) = 2t_a \cos(k_x) + 2t_b \cos(k_y)$.

II. BAND STRUCTURE OF H^{FH} FOR $\delta \neq 0$

This section shows the behavior of individual levels of the Hamiltonian H^{FH} when the parameter ϵ is varied,

in the anisotropic case $t_a \neq t_b$. Periodic boundary conditions were imposed and the diagonalization carried out for four extremal points in \vec{K} space – $(0, 0)$, $(\pi, 0)$, $(0, \pi)$ and (π, π) in dimensionless units. This transition represents a variant of the Lifshitz transition of the type discussed in [23]. At such crossings, states become delocalized along one direction, namely parallel to the chains. We have seen in the main text using a series expansion that the main gap crossing should occur approximately for $\epsilon_c = |2\delta/(3+2\delta)| = \delta/(\frac{3}{2} + \delta)$. This leads to a conjecture – that for larger approximants the transition should occur for

$$\epsilon_c = \left| \frac{\delta}{\tau + \delta} \right| \quad (14)$$

where $\tau = \lim_{k \rightarrow \infty} F_k/F_{k-1}$ is the golden mean.

Fig.4a) shows results obtained for the $k = 4$ approximant. This is a system having 125 sites in its magnetic unit cell. The parameter $\delta = 0.5$. Data for the critical value $\epsilon = \epsilon_c$ in the case of the main gap is plotted in Fig.4b) for two different approximants ($k = 4, 5$). Level-crossings across the four band gaps are shown outlined in black. Fig.4b) is a plot of ϵ_c for the largest bandgap versus the renormalized hopping amplitude t_b for different system sizes. One observes that the data are well fitted by the conjectured expression Eq.14, which is shown by the grey dashed line in the figure. The orange dashed line

is the expression obtained by the power law expansion for $k = 3$ system that we discussed in the main text.

III. RECTANGULAR UNIT CELLS FOR APPROXIMANT STRUCTURES.

To study edge states we have considered rectangular unit cells whose edges lie parallel to the x' and y' axes. The periodicity of the system along the x' axis is unchanged – the structure repeats after F_k sites. However the periodicity along y' is larger by a factor F_k times. If we consider an approximant of slope F_{k-2}/F_{k-1} the two lattice vectors are $\vec{A} = (F_{n-1}, F_{n-2})$ (oriented along the x' axis) and $\vec{B} = F_k(-F_{k-2}, F_{k-1})$ (along the y' axis). The magnetic unit cell is obtained by taking 5 copies of this cell along the x' direction. This is the square cell shown in Fig.3a) of the main text.

An example of a rectangular cell is shown in Fig.5 for the approximant $k = 4$ of 5 sites. The unit cell contains 13 parallel Fibonacci approximant chains – shown in blue – coupled to each other (when ϵ is finite). As can be seen from the figure, when the boundaries along the long edges are opened, these finite chains can differ from each other by an origin shift. Thus, in the 1D limit, edge states appear in the gaps at different energies for different chains of the open system.

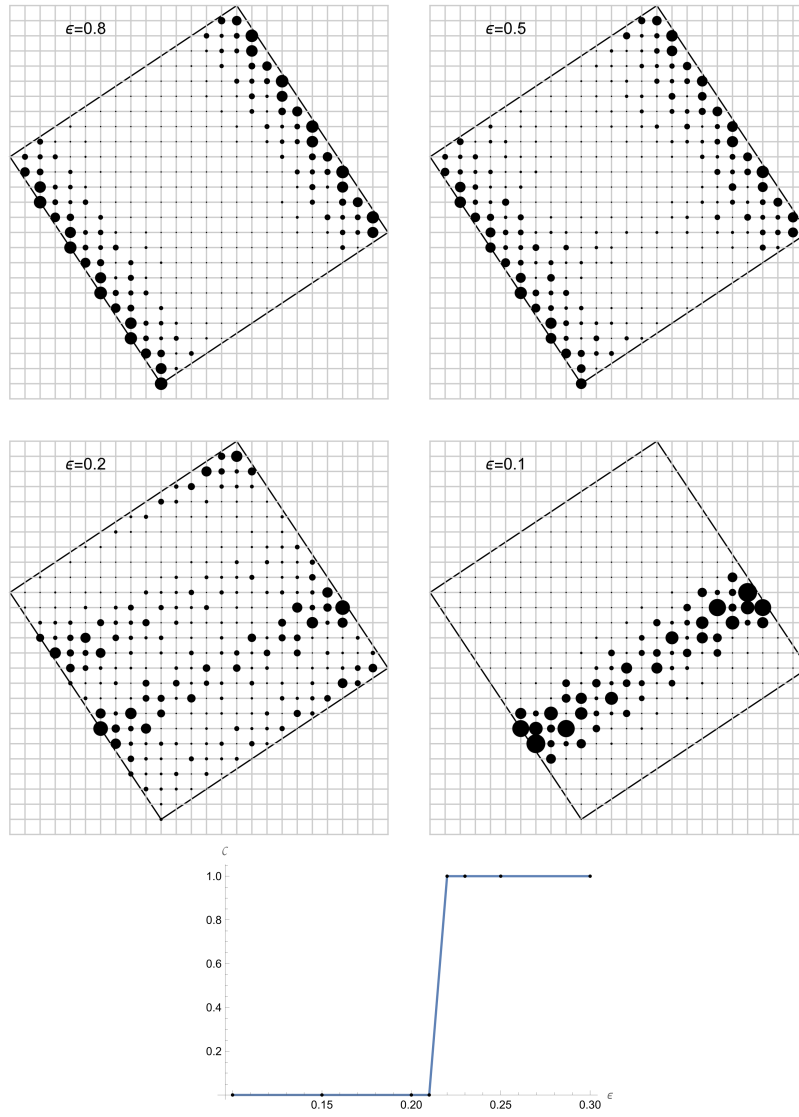


FIG. 3. top) The evolution of an edge state within one of the two largest gaps for the 5-band approximant as ϵ is varied. A square unit cell for the $N = 5$ approximant is taken, and periodic boundary conditions are imposed along the y' direction and $\delta = 0.4$. The radii of the circles at each site are determined by the amplitudes of the wavefunction. It is well-localized for values of ϵ close to 1, and extends into the bulk as ϵ gets smaller. Below the transition, the state resembles a 1D bulk state tending, as $\epsilon \rightarrow 0$ towards a 1D edge state. bottom) The transition in total Chern number of the occupied bands for the same value of $\delta = 0.4$, showing the jump between its value of 1 and the value 0 which occurs at $\epsilon_c \approx 0.2$.

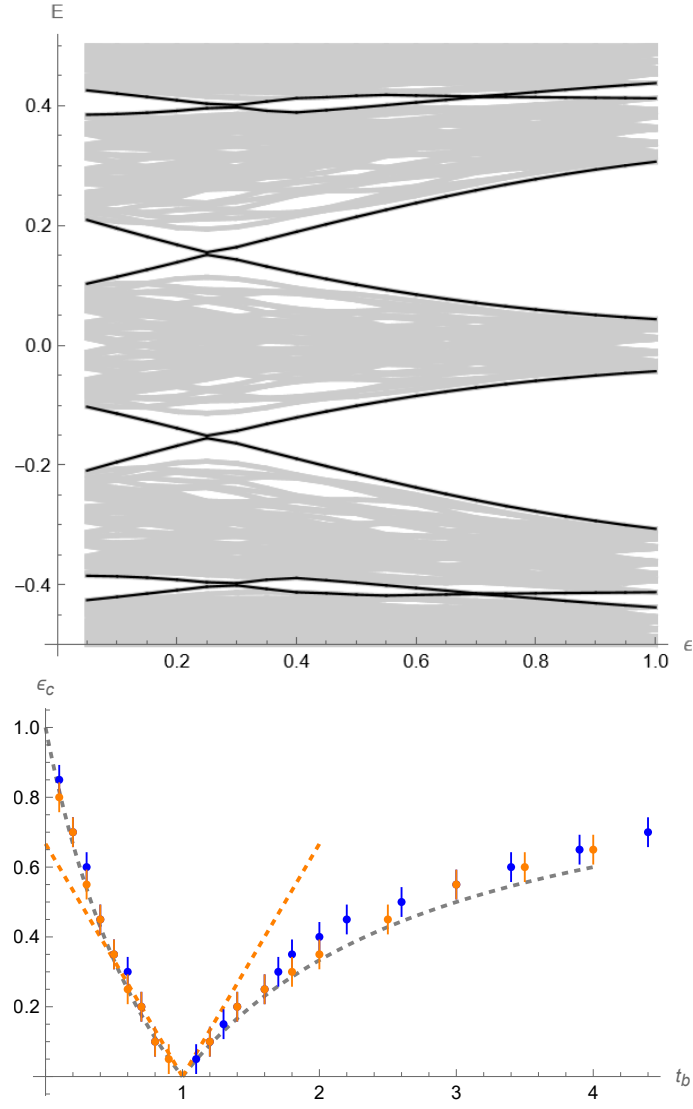


FIG. 4. top) The evolution of energy levels of H^{FH} for fixed $\delta = 0.5$ as a function of ϵ , showing crossings. Data was obtained for $k = 4$ approximant (125 site magnetic unit cell), for four points $(0, 0)$, $(\pi, 0)$, $(0, \pi)$ and (π, π) in reciprocal space. Level-crossings across the four band gaps are shown outlined in black. The band width has been normalized to unity. bottom) Plot of the critical values ϵ_c versus the renormalized hopping amplitude t_b . Blue points are data for $k = 4$, orange points are data for $k = 5$. The orange dashed line is the theoretical expression obtained by series expansion of $k = 3$ model. The grey dashed line is the conjecture of Eq.14.

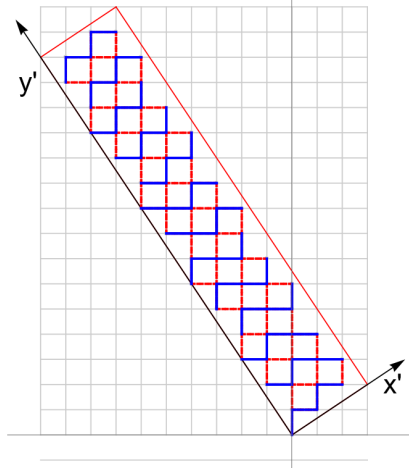


FIG. 5. A unit cell with rectangular form for $k = 4$ approximant, having 13 parallel chains of 5 sites. Blue (red) bonds show intra (inter)chain hoppings between sites. The magnetic unit cell is obtained by taking 5 copies of this cell along the x' direction.